

Size Constraint on Hayabusa2 Extended Mission Rendezvous Target 1998 KY₂₆ via VLT/VISIR Non-detection

JIN BENIYAMA ^{1,2} THOMAS G. MÜLLER ³ MARCO DELBO ^{1,4} ERIC PANTIN ⁵ OLIVIER R. HAINAUT ⁶
MARCO MICHELI ⁷ AND MICHAËL MARSETT ⁸

¹ *Université Côte d'Azur, Observatoire de la Côte d'Azur, CNRS, Laboratoire Lagrange, Bd de l'Observatoire, CS 34229, 06304 Nice Cedex 4, France*

² *Institute of Astronomy, Graduate School of Science, The University of Tokyo, 2-21-1 Osawa, Mitaka, Tokyo 181-0015, Japan*

³ *Max-Planck-Institut für extraterrestrische Physik, Giessenbachstraße, Postfach 1312, 85741 Garching, Germany*

⁴ *School of Physics and Astronomy, University of Leicester, Leicester LE1 7RH, UK*

⁵ *Université Paris-Saclay, Université Paris Cité, CEA, CNRS, AIM, 91191, Gif-sur-Yvette, France*

⁶ *European Southern Observatory, Karl-Schwarzschild-Straße 2, 85748 Garching-bei-München, Germany*

⁷ *ESA NEO Coordination Centre, Planetary Defence Office, Largo Galileo Galilei 1, I-00044 Frascati (RM), Italy*

⁸ *European Southern Observatory, Alonso de Córdova 3107, Santiago, Chile*

(Received February 25, 2025; Revised March 20, 2025)

Submitted to AJ

ABSTRACT

1998 KY₂₆ is a tiny near-Earth asteroid ($H = 26.1$) discovered in 1998. It has been selected as the target of the Hayabusa2 extended mission, which will rendezvous with 1998 KY₂₆ in 2031. However, one of the most basic physical properties, size, remains poorly constrained, posing potential challenges for spacecraft operations. We aimed at constraining the size of 1998 KY₂₆ by means of thermal infrared observations. We performed thermal infrared observations of 1998 KY₂₆ using the ESO Very Large Telescope/VISIR on three consecutive nights in May 2024. After stacking all frames, we find no apparent detection of 1998 KY₂₆ on the resulting images. The upper-limit flux density of 1998 KY₂₆ is derived as 2 mJy at 10.64 μm . From this upper-limit flux density obtained via non-detection, we conclude that the diameter of 1998 KY₂₆ is smaller than 17 m with thermophysical modeling. This upper limit size is smaller than the radar-derived 30 (± 10) m. Our size constraint on 1998 KY₂₆ is essential for the operation of the Hayabusa2 spacecraft during proximity operations using remote sensing instruments as well as a possible impact experiment using the remaining projectile.

Keywords: Asteroids (72) — Near-Earth Objects(1092) — Photometry (1234)

1. INTRODUCTION

The Hayabusa2 spacecraft finished its main mission, the exploration of the near-Earth asteroid (NEA) (162173) Ryugu in 2020, after dedicated in situ remote-sensing measurements and experiments as well as a successful sample return (e.g., Sugita et al. 2019; Watanabe et al. 2019; Kitazato et al. 2019). Currently, Hayabusa2 is in the cruise phase of its extended mission, which will consist in visiting two more NEAs. Recently, 1998 KY₂₆ has been selected as the rendezvous target of the Hayabusa2 extended mission (Hirabayashi et al. 2021; Kikuchi et al. 2023). The

spacecraft will firstly flyby with (98943) Torifune (a.k.a. 2001 CC₂₁) in 2026, and rendezvous with 1998 KY₂₆ in 2031.

1998 KY₂₆ is an NEA discovered by the Spacewatch project in Arizona, US on 1998 May 28¹ (McMillan & Spacewatch Team 2007). Quick response observations of 1998 KY₂₆ soon after its discovery were performed in June 1998: radar observations using the Goldstone Solar System Radar and photometric observations with four small aperture ($D \leq 1$ m) telescopes (Ostro et al. 1999). From the optical photometry, a rotation period of 1998 KY₂₆ was derived as $P = 10.7015 \pm 0.0004$ minutes (1σ error), and color indices were derived as $B - R = 0.083 \pm 0.070$,

Corresponding author: Jin Beniyama
jbeniyama@oca.eu

¹ <https://www.minorplanetcenter.net/mpec/J98/J98L02.html>

$V - R = 0.058 \pm 0.055$, and $R - I = 0.088 \pm 0.053$ (1σ error with solar colors subtracted). From the color indices as well as geometric albedo derived from their radar-derived diameter and absolute magnitude, they inferred that 1998 KY₂₆ belongs to B-, C-, F-, G-, D-, P-, or M-type asteroids in Tholen taxonomy (Tholen 1984). Since the radar albedo of 1998 KY₂₆ is not consistent with that of typical M-type asteroids, a classification as B-, C-, F-, G-, D-, or P-type was favored (Ostro et al. 1999).

The radar echo spectra, together with the derived rotation period, were used to estimate the 1998 KY₂₆'s shape and size. Considering the uncertainties of its pole orientation, Ostro et al. (1999) estimated the effective diameter of 1998 KY₂₆ to be 30 (± 10) m. The circular-polarization ratios (SC/OC ratios) of 1998 KY₂₆ were derived to be 0.5 ± 0.1 , which exceeds 90% of the SC/OC ratios of NEAs at the time of the publication.

The Hayabusa2 extended mission gives us an exceptional opportunity to compare and test our knowledge of tiny asteroids obtained with telescopic and in situ observations. However, no detailed physical characterizations of 1998 KY₂₆ have ever been done except for colors, shape model, and rotation period (Ostro et al. 1999), simply due to the observational difficulties and poor observational opportunities. As written by Ostro et al. (1999), it is still unclear whether tiny asteroids are *coherent solid rocks or gravitationally bound, multicomponent agglomerates*; 1998 KY₂₆ is a potential target to answer this question. Moreover, Seligman et al. (2023) reported unexpected large out-of-plane nongravitational accelerations for seven NEAs including 1998 KY₂₆. One possibility is that some fractions of small NEAs are extinct "dark comets" in the near-Earth space. Future characterizations are essential to examine the dynamical evolution of such a new population. The determination of the diameter of 1998 KY₂₆ with an independent technique is therefore greatly desired to prepare and maximize the outcomes of the in situ measurements by the Hayabusa2 extended mission in 2031.

In this paper, we report the results of thermal infrared observations of 1998 KY₂₆ in May 2024. The paper is organized as follows. In Section 2, we describe our thermal infrared observations and data reduction with VLT/VISIR. The results of the observations are presented in Section 3. The constraints on the physical properties of 1998 KY₂₆ and the implications for the Hayabusa2 extended mission are discussed in Section 4.

2. OBSERVATIONS AND DATA REDUCTION

An attempt to detect 1998 KY₂₆ at thermal infrared wavelengths was conducted in May 2024. As part of the ESO observing program "Thermal Observations of the Hayabusa2 Extended Mission Target Asteroid 1998 KY₂₆" (113.26MY, PI: J. Beniyama), we conducted measurements in the N-band

filters B8.7, B10.7, and B11.7 on three consecutive nights (2024 May 26, 27, and 28 UT). The observing conditions are summarized in Table 1.

We performed thermal infrared imaging observations using the VLT spectrometer and imager for the mid-infrared (VISIR, Lagage et al. 2004) located at the Cassegrain focus of Unit Telescope 2 of the ESO Very Large Telescope (VLT) on Cerro Paranal, Chile. VISIR provides imaging at high-sensitivity in two mid-infrared atmospheric windows: the N-band between ≈ 8 to 13 μm and the Q-band between ≈ 16.5 to 24.5 μm . VLT/VISIR reaches diffraction-limited images at ~ 0.3 arcsec full width at half maximum (FWHM) in the N-band.

VISIR has a $1\text{k} \times 1\text{k}$ Raytheon Aquarius IBC detector (1024×1024 pixel). The field of view is 38.0 arcsec \times 38.0 arcsec with a pixel scale of 0.045 arcsec pixel⁻¹. The observations of all standard stars were done in the perpendicular nod-chop mode with a throw of 8 arcsec, while the observations of 1998 KY₂₆ were done in the parallel nod-chop mode with a throw of 8 arcsec, which is recommended for faint sources.

The observing sequence with calibration stars interleaved with our science target covered more than 3 hours each night. The effective on-source integration times are between 15 and 18 minutes in each filter. All measurements were taken in sky conditions with V-band seeing below or around 1.4 arcsec, precipitable water vapor (PWV) levels well below 5 mm H₂O, and with the target seen under an airmass below 1.25. Chopping frequencies were set to ~ 4 Hz. Although the Srehl ratio was in the range 0.4–0.5, the PSF FWHM was maintained to less than 0.4 arcsec.

1998 KY₂₆ was observed in non-sidereal tracking with blind preset and offset speed from VLT-centric 1998 KY₂₆ ephemeris provided by JPL Horizons², using observatory code 309 for Paranal. Since 1998 KY₂₆ was recovered on 2024 April 17³ before our observations, its updated orbit was accurate at the ≤ 1 arcsec level during our observing runs. The absolute pointing accuracy of the VLT is set by its pointing model, which is better than 3 arcsec RMS. For all observations, it is further refined by the acquisition of a guide star, bringing the pointing accuracy to that of the star's position (typically better than 1 arcsec, even considering that its proper motion is not accounted for by the VLT). An additional source of pointing uncertainty is the time difference between the ephemerides time-stamp used and the time at which the telescope reaches that position and starts tracking at non-sidereal rates. While the goal is to keep that difference below a few seconds it can, in some cases, reach 10 or

² <https://ssd.jpl.nasa.gov/horizons>

³ <https://minorplanetcenter.net/mpec/K24/K24H23.html>

even 20 s. Accounting for the apparent motion of the object (800 arcsec/h at the time of the observations, or 0.22 arcsec/s), this could cause a pointing error of up to 4–5 arcsec. Overall, we are therefore confident that the object was well within VISIR’s field of view. As tracking accuracy is exquisite (VLT performance webpage⁴) and as the telescope was kept locked on its guide star during the observations, we are therefore confident that the object remained at a small (<4–5 arcsec), constant, offset from the expected position. Co-adding the images blindly relying on the telescope position therefore does not degrade the image quality of the stack.

The data were initially processed using a private and customized version of the VISIR pipeline (Pantin 2010). For every day/filter dataset, the chopping and nodding offset frames are combined to produce a single frame in which the different “beams” are supposed to be. The observations were performed in the so-called “parallel mode” in which the signal is spread on the detector, with a central positive beam containing half of the total source flux and two negative beams symmetrically apart from the central beam (Pantin 2010). At that stage, no point source is identifiable in the resulting frames. Yet, since the secondary mirror (chopper) and telescope nodding offsets are known from the telemetry, it is possible to blindly combine the beams by applying the adequate frames offsets and sum. This final image is radiometrically calibrated using the conversion factor from ADU to Jy deduced from the standard star observations obtained before or after 1998 KY₂₆.

3. RESULTS

We performed thermal observations with VLT/VISIR on three consecutive nights. After the operations described in Section 2, one is searching for a single point source that could be 1998 KY₂₆. Its position on the detector cannot be perfectly known since a blind telescope absolute preset is only accurate to a few arcsec. From the noise only, it is possible to assess a point source sensitivity. These sensitivities are given in Table 2. None of the final reduced images in any filter/night is at first sight showing any presence of a point source that would correspond to 1998 KY₂₆. In order to search deeper, the following procedure has been applied. For a given filter among the three selected for the observations, the best observation in terms of sensitivity is selected. It turned out that since the second night (2024 May 27) was the best one, all the selected observations come from this night. This image is then convolved with the center symmetric version of the PSF, which is equivalent to the correla-

tion product with the PSF. This corresponds to the so-called optimal or “matched filtering”. This linear filtering allows to optimally increase the SNR and the chances of detection. The corresponding point source detectivities, deduced from visual detection of the synthetic point sources with varying fluxes, are given in Table 2. Despite this processing, no point source can be identified in any of the filtered datasets. In order to double-check visually the point sources detectivities deduced only from the noise measure, we also included synthetic point sources in the datasets. 5, 3, 2, and 1.5 mJy point sources were artificially added to the frames (before matched filtering) using the measured PSFs. Figure 1 displays the frames in the B10.7 most sensitive filter (2024 May 27) before filtering and after. Before filtering, the 1.5 mJy, 2 mJy, and 3 mJy sources are barely detectable; after filtering, the 2 mJy and 3 mJy sources become fairly detectable; which we consider as our detection upper limit.

4. DISCUSSION

Despite the good weather conditions, 1998 KY₂₆ was not detected. The object’s fast rotation and the three-nights repeated multi-band observing sequences spanning much longer than the rotation period make it also unlikely that we saw each time only the minimum cross-section of an elongated body. The most-constraining non-detection limit from the VISIR measurement is related to the B10.7 measurements from 2024 May 27; the optimum filtered images would have shown 1998 KY₂₆ if the object had a flux density of 2 mJy or higher (see Section 3).

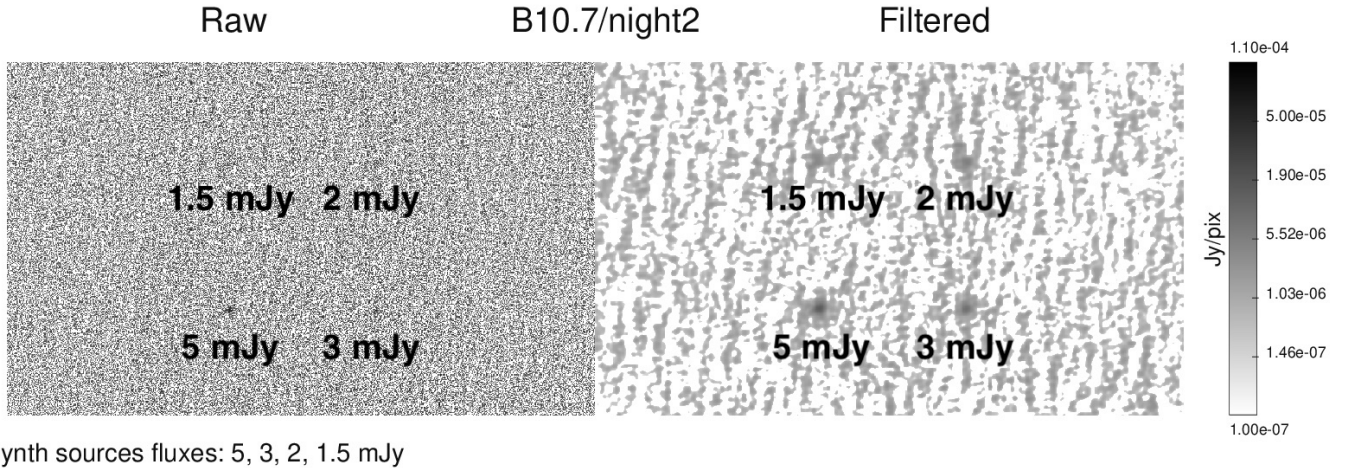
We calculated for this specific epoch, and the B10.7 reference wavelength at 10.64 μm , a range of thermal model predictions to see if the non-detection limit can tell us something about 1998 KY₂₆’s physical and thermal properties. We started with the fast rotating model (FRM, Lebofsky & Spencer 1989, and references therein) which has a temperature distribution that is isothermal in longitude and depends on the latitude. The use of the FRM in this case can be justified by the object’s very short rotation period. In parallel, we also used the near-Earth asteroid thermal model (NEATM, Harris 1998), using beaming parameters of $\eta = 1.0$ and 1.5 to account for the large phase angle ($\alpha = 45^\circ$ on 2024 May 27). In addition, we used a more sophisticated thermophysical model (TPM), which is based on the work by Lagerros (1996, 1998); Müller (2002). The TPM allows to use of arbitrary spin-shape solutions, and considers a one-dimensional heat conduction into the surface, self-heating and shadowing effects due to surface topography and roughness for the true solar illumination and observing geometries as seen by VISIR. Surface roughness is modelled by means of different parametrizations, either as hemispherical segments or as ran-

⁴ <https://www.eso.org/sci/facilities/paranal/telescopes/ut/utperformance.html>

Table 1. Summary of the observations

Starting Time (UTC)	Object	Filter	t_{exp} (s)	N_{img}	V (mag)	α (deg)	Δ (au)	r_{h} (au)	Airmass	Sky	V seeing (arcsec)	MIR seeing (arcsec)
2024-05-26 06:11:44	HD 145897	B10.7	59.994	2	5.239				1.11–1.11	PH	1.0	0.3
06:48:42	1998 KY ₂₆	B10.7	101.772	20	20.2	41.4	0.036	1.040	1.04–1.05	PH	1.1	
07:44:41	HD 187150	B8.7	59.994	2	6.46				1.03–1.03	PH	1.0	0.3
07:55:00	1998 KY ₂₆	B8.7	103.95	20	20.2	41.5	0.036	1.040	1.04–1.08	PH	1.2	
08:50:52	1998 KY ₂₆	B11.7	93.5712	20	20.2	41.6	0.036	1.040	1.10–1.18	PH	1.0	
09:44:11	HD 216149	B11.7	60.1236	2	5.4				1.10–1.10	PH	0.9	0.4
2024-05-27 05:12:33	HD 133774	B11.7	60.1236	2	5.2				1.11–1.11	PH	1.3	0.4
05:21:58	1998 KY ₂₆	B11.7	93.5712	20	20.2	44.4	0.035	1.038	1.14–1.25	PH	1.2	
06:07:13	1998 KY ₂₆	B8.7	103.95	20	20.2	44.5	0.035	1.038	1.06–1.13	PH	1.3	
07:11:10	HD 187150	B8.7	59.994	2	6.46				1.06–1.06	PH	1.3	0.3
07:14:41	HD 187150	B10.7	59.994	2	6.46				1.05–1.05	PH	1.3	0.3
07:20:28	1998 KY ₂₆	B10.7	101.772	20	20.2	44.7	0.035	1.038	1.04–1.04	PH	1.4	
2024-05-28 06:24:13	HD 163376	B10.7	59.994	2	4.863				1.05–1.05	CL	0.7	0.3
06:41:17	1998 KY ₂₆	B10.7	101.772	20	20.2	48.2	0.033	1.035	1.05–1.10	TN	0.7	
07:35:13	1998 KY ₂₆	B11.7	93.5712	20	20.2	48.3	0.033	1.035	1.04–1.05	TN	0.9	
08:21:21	1998 KY ₂₆	B8.7	103.95	20	20.2	48.4	0.033	1.035	1.05–1.08	CL	0.8	
09:21:07	HD 189831	B11.7	60.1236	2	4.764				1.05–1.05	CL	1.0	0.3
09:24:35	HD 189831	B8.7	59.994	2	4.764				1.06–1.06	CL	1.0	0.3

NOTE— The observation time in UT at the starting-time of exposure (Starting Time), target of observations (Object), filters (Filter), total exposure time (t_{exp}), number of images (N_{img}), and V-band apparent magnitude (V) are listed. The phase angle (α), distance between 1998 KY₂₆ and observer (Δ), and distance between 1998 KY₂₆ and the Sun (r_{h}) at the observation starting time were from NASA JPL Horizons on 2025 January 10. Elevations of 1998 KY₂₆ used to calculate the airmass range (Airmass) are also from NASA JPL Horizons. Sky condition (Sky, PH: Photometric, CL: Clear, TN: Thin cirrus) and seeing FWHM at 500 nm and zenith (V Seeing) are from the VLT UT2 Service Telescope Reports. Seeing FWHM of the standard observations (MIR seeing) are derived by fitting light-intensity profiles with Moffat functions.



Synth sources fluxes: 5, 3, 2, 1.5 mJy

Figure 1. Final stacked image with synthetic point source objects with flux densities of 5 mJy, 3 mJy, 2 mJy, and 1.5 mJy inserted. The flux density of the synthetic sources are indicated in the accompanying text.

dom Gaussian surfaces. The model parameters for the FRM, the NEATM, and the TPM are listed in Table 3. It is known that a rotation period determined from only one apparition has some ambiguity especially if the shape is not very elongated as 1998 KY₂₆ (e.g., Harris et al. 2014). We used the TPM with a rotation period of 5.35 minutes, which is twice as

fast as that reported in Ostro et al. (1999). It was determined by a recent study on lightcurves of 1998 KY₂₆ (T. Santana-Ros et al. 2025, in review). We used a spherical shape in the TPM, which is justified with the long integration time and the short rotation period of 1998 KY₂₆; we measured the rotational-averaged signal.

Table 2. Measured point source sensitivities in units of mJy/10 σ on the various datasets.

	2024 May 26	2024 May 27	2024 May 27	2024 May 28
	Raw	Raw	Filtered	Raw
B8.7	4.46	4.20	2.00	5.34
B10.7	4.53	4.46	2.50	5.42
B11.7	5.91	5.66	3.00	6.46

NOTE— "Raw" refers to the final image after pipeline processing, while "Filtered" refers to the same image after matched filtering (see the text).

The highest fluxes are obtained in case of a pole-on viewing geometry and a low albedo of $p_V = 0.05$, where the thermal inertia have very little influence, see Figure 2. The prograde equator-on geometry in combination with a low albedo and a low thermal inertia produced similar-level fluxes. The retrograde equator-on geometry in combination with a high albedo ($p_V=0.6$) and a high thermal inertia (here $\Gamma=300 \text{ J m}^{-2} \text{ s}^{-0.5} \text{ K}^{-1}$) gave the lowest fluxes. Higher thermal inertia, or a smooth surface (instead of a low-roughness surface) would lower the fluxes a few percent and push them into the regime of the FRM predictions. The FRM predictions, at this phase angle of about 45° , produced the lowest fluxes for a given object size. These values are considered as absolutely lowest flux boundary, however, there is no evidence that small, fast-rotating asteroids are following the isothermal temperature distributions of the FRM. Recently, the thermal inertia of two fast-rotating small asteroids like 1998 KY₂₆ was reported as low as $10\text{--}100 \text{ J m}^{-2} \text{ s}^{-0.5} \text{ K}^{-1}$ (Fenucci et al. 2021, 2023), though this is still not conclusive since the sample is limited. The NEATM predictions are between the highest and lowest fluxes.

On the basis of Figure 2, we conclude that 1998 KY₂₆ has to be smaller than 17 m otherwise our VISIR measurements would have detected the asteroid. This value is smaller than the radar-derived $30 (\pm 10) \text{ m}$ by Ostro et al. (1999). Our upper size limit of 1998 KY₂₆ is consistent with a recent study on lightcurves and a re-interpretation of the radar measurements (T. Santana-Ros et al. 2025, in review), which indicates that 1998 KY₂₆ is truly smaller than the size estimated in Ostro et al. (1999). The thermal infrared flux is driven by the size of the object and its surface temperature, which has a weak dependence on geometric albedo. Thus, it is difficult to constrain geometric albedo with our non-detection.

Mommert et al. (2014) constrained physical and thermal properties of another tiny NEA 2009 BD ($H = 28.4$) from Spitzer Space Telescope/Infrared Array Camera (IRAC) non-detection at $4.5 \mu\text{m}$. They did not detect the target within 25 hr of integration. They performed a TPM of 2009 BD as in our case. Additionally, they model two nongravitational effects, solar radiation pressure and the Yarkovsky

effect, to constrain parameters such as size, thermal inertia, mass density, and obliquity (i.e., spin orientation). The combination of the two models gave stronger constraints on the physical properties of asteroids. An unexpectedly large out-of-plane nongravitational acceleration was reported for 1998 KY₂₆ (Seligman et al. 2023, which posed the possibility that 1998 KY₂₆ is a dark comet), which add further complexity to the model.

Kareta & Moskovitz (2024) reported multi-filter photometry of 1998 KY₂₆ in the visible wavelength with the 4.3 m Lowell Discovery Telescope. They showed that 1998 KY₂₆ has a D-type reflectance spectrum, which might have primitive organic materials on the surface (Barucci et al. 2018). A typical geometric albedo of D-types is estimated as ~ 0.06 for asteroids with the diameter of $D \geq 10 \text{ km}$ (Usui et al. 2013), while recently it was reported to be ~ 0.04 for NEAs observed by the MIT-Hawaii NEO Spectroscopic Survey (Marsset et al. 2022). However, a caveat is that a typical albedo value for D-type NEAs with the diameter of $D \leq 20 \text{ m}$ as 1998 KY₂₆ is unclear since the number of samples is limited.

On the other hand, it is possible to constrain the lower limit of the geometric albedo of 1998 KY₂₆ from our upper size limit and the updated absolute magnitude of $H = 26.13 \pm 0.16$, which was derived from an extensive photometric study covering a wide range of solar phase angles and geometries (T. Santana-Ros et al. 2025, in review). The geometric albedo of 1998 KY₂₆ is estimated to be ≥ 0.19 with $H = 26.29$ and $D \leq 17 \text{ m}$, which is significantly larger than the typical geometric albedo of D-types. The large geometric albedo of 1998 KY₂₆ is consistent with a recent Xe-type classification in Bus-DeMeo taxonomy (Bolin et al. 2025). Spectroscopic observations in wide wavelength coverage are essential to further investigate the surface composition of 1998 KY₂₆.

Our size constraint on 1998 KY₂₆ affects the operation of Hayabusa2 spacecraft. A tight size constraint is obviously important during proximity operations using remote sensing instruments since pixel resolution and spatial resolution are essential in determination of the spacecraft's orbit. More-

over, the Hayabusa2 spacecraft has a tantalum projectile on it (Kikuchi et al. 2023). An impact experiment using the remaining projectile would be an option for the extended mission at 1998 KY₂₆, though a potential use of the projectile is under discussion (Hirabayashi et al. 2021). Given a fixed bulk density and smaller size, an expected crater diameter might be larger.

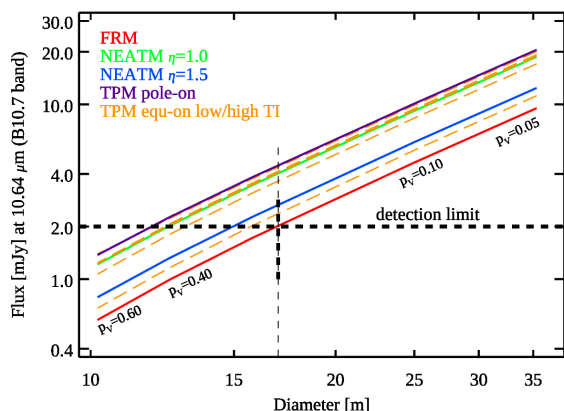


Figure 2. Flux predictions (in mJy for 1998 KY₂₆ for 2024 May 27 based on different model assumptions and for a wide range of object sizes. The VISIR/B10.7 band point-source detection limit is indicated as a horizontal dashed line. The various model parameters are explained in the text.

5. CONCLUSIONS

We performed thermal observations of 1998 KY₂₆, the Hayabusa2 extended mission rendezvous target, with

VLT/VISIR in May 2024. From the upper limit flux density via non-detection with VLT/VISIR, we constrained that the diameter of 1998 KY₂₆ is smaller than 17 m through the TPM, which is smaller than the radar-derived diameter. Our size constraint on 1998 KY₂₆ is crucial for the operation of Hayabusa2 spacecraft during proximity operations using remote sensing instruments and a possible impact experiment using the remaining projectile on the spacecraft.

We acknowledge the anonymous referee for a constructive report that improved the quality of the paper. We thank Dr. Bruno Leibundgut, the Director of the ESO for Science, for the time allocation to observe 1998 KY₂₆. The authors are grateful to Dr. Makoto Yoshikawa and Dr. Toshi Hirabayashi for supporting this project. We thank Dr. Mario van den Ancker for observing assistance with VLT/VISIR. J.B. thanks Dr. Shigeyuki Sako and Dr. Takafumi Kamizuka for the discussion of thermal observations. We are grateful to Dr. Konrad R. W. Tristram, Dr. Bin Yang, and Dr. Julia V. Seidel for valuable comments on VLT/VISIR observations and data reduction. This work is based on observations collected at the European Southern Observatory under ESO programme 113.26MY (PI: J. Beniyama) This work was supported by JSPS KAKENHI Grant Numbers JP22K21344 and JP23KJ0640. Last but certainly not least, J.B. would like to thank support from the Hayakawa Satio Fund awarded by the Astronomical Society of Japan for giving the opportunity to work on this project.

Facilities: VLT:Kueyen (VISIR)

Software: NumPy (Oliphant 2015; Harris et al. 2020), pandas (Reback et al. 2021), SciPy (Virtanen et al. 2020), AstroPy (Astropy Collaboration et al. 2013, 2018), astroquery (Ginsburg et al. 2019)

REFERENCES

- Astropy Collaboration, Robitaille, T. P., Tollerud, E. J., et al. 2013, *A&A*, 558, A33, doi: [10.1051/0004-6361/201322068](https://doi.org/10.1051/0004-6361/201322068)
- Astropy Collaboration, Price-Whelan, A. M., Sipőcz, B. M., et al. 2018, *AJ*, 156, 123, doi: [10.3847/1538-3881/aabc4f](https://doi.org/10.3847/1538-3881/aabc4f)
- Barucci, M. A., Perna, D., Popescu, M., et al. 2018, *MNRAS*, 476, 4481, doi: [10.1093/mnras/sty352](https://doi.org/10.1093/mnras/sty352)
- Bolin, B. T., Fremling, C., Belyakov, M., et al. 2025, arXiv e-prints, arXiv:2501.17156, doi: [10.48550/arXiv.2501.17156](https://doi.org/10.48550/arXiv.2501.17156)
- Fenucci, M., Novaković, B., & Marčeta, D. 2023, *A&A*, 675, A134, doi: [10.1051/0004-6361/202346160](https://doi.org/10.1051/0004-6361/202346160)
- Fenucci, M., Novaković, B., Vokrouhlický, D., & Weryk, R. J. 2021, *A&A*, 647, A61, doi: [10.1051/0004-6361/202039628](https://doi.org/10.1051/0004-6361/202039628)
- Ginsburg, A., Sipőcz, B. M., Bressier, C. E., et al. 2019, *AJ*, 157, 98, doi: [10.3847/1538-3881/aafc33](https://doi.org/10.3847/1538-3881/aafc33)
- Harris, A. W. 1998, *Icarus*, 131, 291, doi: [10.1006/icar.1997.5865](https://doi.org/10.1006/icar.1997.5865)
- Harris, A. W., Pravec, P., Galád, A., et al. 2014, *Icarus*, 235, 55, doi: [10.1016/j.icarus.2014.03.004](https://doi.org/10.1016/j.icarus.2014.03.004)
- Harris, C. R., Millman, K. J., van der Walt, S. J., et al. 2020, *Nature*, 585, 357, doi: [10.1038/s41586-020-2649-2](https://doi.org/10.1038/s41586-020-2649-2)
- Hirabayashi, M., Mimasu, Y., Sakatani, N., et al. 2021, *Advances in Space Research*, 68, 1533, doi: [10.1016/j.asr.2021.03.030](https://doi.org/10.1016/j.asr.2021.03.030)
- Kareta, T., & Moskovitz, N. 2024, in *AAS/Division for Planetary Sciences Meeting Abstracts*, Vol. 56, AAS/Division for Planetary Sciences Meeting Abstracts, 208.02
- Kikuchi, S., Mimasu, Y., Takei, Y., et al. 2023, *Acta Astronautica*, 211, 295, doi: [10.1016/j.actaastro.2023.06.010](https://doi.org/10.1016/j.actaastro.2023.06.010)
- Kitazato, K., Milliken, R. E., Iwata, T., et al. 2019, *Science*, 364, 272, doi: [10.1126/science.aav7432](https://doi.org/10.1126/science.aav7432)

Table 3. Thermal model parameter space for predicting KY₂₆ fluxes for 2024 May 27 08:00 at the VISIR/B10.7 reference wavelengths of 10.64 μm .

Model	parameter space
FRM	$r = 1.038 \text{ au}$, $\Delta = 0.0346 \text{ au}$
NEATM	$r = 1.038 \text{ au}$, $\Delta = 0.0346 \text{ au}$, $\alpha = 44.7^\circ$ beaming parameter $\eta = 1.0$ and 1.5
TPM	$r = 1.038 \text{ au}$, $\Delta = 0.0346 \text{ au}$, $\alpha = 44.7^\circ$ size (effective diameter) range: 10 ... 35 m geometric V-band albedo p_V : 0.05 ... 0.6 $H = 26.13$, $G = 0.15$ roughness (rms of surface slopes): 5 ... 20° thermal inertia Γ : 30 ... 300 $\text{J m}^{-2} \text{s}^{-0.5} \text{K}^{-1}$ rotation period P : 5.35 min different spin-vector orientations: (1) prograde, equator-on: $(\lambda, \beta) = (111.2^\circ, +77.1^\circ)$ (2) retrograde, equator-on: $(\lambda, \beta) = (291.2^\circ, -77.1^\circ)$ (3) pole-on: $(\lambda, \beta) = (291.2^\circ, +12.9^\circ)$

NOTE— H is the latest value derived from an extensive photometric study (see the text).

- Lagage, P. O., Pel, J. W., Authier, M., et al. 2004, *The Messenger*, 117, 12
- Lagerros, J. S. V. 1996, *A&A*, 310, 1011
- Lagerros, J. S. V. 1998, *A&A*, 332, 1123
- Lebofsky, L. A., & Spencer, J. R. 1989, in *Asteroids II*, ed. R. P. Binzel, T. Gehrels, & M. S. Matthews, 128–147
- Marsset, M., DeMeo, F. E., Burt, B., et al. 2022, *AJ*, 163, 165, doi: [10.3847/1538-3881/ac532f](https://doi.org/10.3847/1538-3881/ac532f)
- McMillan, R. S., & Spacewatch Team. 2007, in *Near Earth Objects, our Celestial Neighbors: Opportunity and Risk*, ed. G. B. Valsecchi, D. Vokrouhlický, & A. Milani, Vol. 236, 329–340, doi: [10.1017/S1743921307003407](https://doi.org/10.1017/S1743921307003407)
- Mommert, M., Hora, J. L., Farnocchia, D., et al. 2014, *ApJ*, 786, 148, doi: [10.1088/0004-637X/786/2/148](https://doi.org/10.1088/0004-637X/786/2/148)
- Müller, T. G. 2002, *M&PS*, 37, 1919, doi: [10.1111/j.1945-5100.2002.tb01173.x](https://doi.org/10.1111/j.1945-5100.2002.tb01173.x)
- Oliphant, T. E. 2015, *Guide to NumPy*, 2nd edn. (North Charleston, SC, USA: CreateSpace Independent Publishing Platform)
- Ostro, S. J., Pravec, P., Benner, L. A. M., et al. 1999, *Science*, 285, 557, doi: [10.1126/science.285.5427.557](https://doi.org/10.1126/science.285.5427.557)
- Pantin, E. 2010, PhD thesis, CEA Saclay, Service d’Astrophysique
- Reback, J., jbrockmendel, McKinney, W., et al. 2021, pandas-dev/pandas: Pandas 1.3.4, v1.3.4, Zenodo, Zenodo, doi: [10.5281/zenodo.5574486](https://doi.org/10.5281/zenodo.5574486)
- Seligman, D. Z., Farnocchia, D., Micheli, M., et al. 2023, *PSJ*, 4, 35, doi: [10.3847/PSJ/acb697](https://doi.org/10.3847/PSJ/acb697)
- Sugita, S., Honda, R., Morota, T., et al. 2019, *Science*, 364, eaaw0422, doi: [10.1126/science.aaw0422](https://doi.org/10.1126/science.aaw0422)
- Tholen, D. J. 1984, PhD thesis, University of Arizona
- Usui, F., Kasuga, T., Hasegawa, S., et al. 2013, *ApJ*, 762, 56, doi: [10.1088/0004-637X/762/1/56](https://doi.org/10.1088/0004-637X/762/1/56)
- Virtanen, P., Gommers, R., Oliphant, T. E., et al. 2020, *Nature Methods*, 17, 261, doi: [10.1038/s41592-019-0686-2](https://doi.org/10.1038/s41592-019-0686-2)
- Watanabe, S., Hirabayashi, M., Hirata, N., et al. 2019, *Science*, 364, 268, doi: [10.1126/science.aav8032](https://doi.org/10.1126/science.aav8032)